Ion cyclotron instability due to the thermal anisotropy of drifting ion species

Article *in* Journal of Geophysical Research Atmospheres · January 2003

DOI: 10.1029/2002JA009576

2 authors, including:

J. A. Valdivia
University of Chile
184 PUBLICATIONS **2,291** CITATIONS

SEE PROFILE

Ion cyclotron instability due to the thermal anisotropy of drifting ion species

L. Gomberoff and J. A. Valdivia

Departamento de Física, Facultad de Ciencias, Universidad de Chile, Chile

Received 8 July 2002; revised 30 October 2002; accepted 25 November 2002; published 31 January 2003.

[1] In a recent study of ion cyclotron waves generated by the thermal anisotropy of oxygen ions, it was shown that the heavy ion drift velocity and a large thermal anisotropy of the heavy ions can destabilize proton-cyclotron waves [*Gomberoff and Valdivia*, 2003]. Here this study is extended to alpha particles in order to show that a much smaller thermal anisotropy is required to trigger strong proton-cyclotron waves. It is also shown that under some conditions, the alpha particle branch of the dispersion relation becomes unstable for frequency values beyond the proton gyrofrequency. This instability occurs for very large alpha particle thermal anisotropy and very low $\beta_{\|\alpha} = v_{th}^2/v_A^2$, where v_{th} and v_A are the thermal and Alfvén velocity, respectively. The maximum growth rate of this branch of the dispersion relation occurs for drift velocities of the alpha particles larger than those that drive the maximum growth rate of the proton-cyclotron instability. Finally, it is demonstrated that the combined effect of oxygen ions and alpha particles lead to a complex unstable spectrum, and to an enhancement of the proton-cyclotron instability. This mechanism is like a cascade effect in which low-frequency ion cyclotron waves can drive unstable high-frequency ion cyclotron waves through anisotropic heating and acceleration of heavy ions. These results may be relevant to the understanding of the heating process of the fast solar wind in coronal holes. *INDEX TERMS:* 7507 Solar Physics, Astrophysics, and Astronomy: Chromosphere; 7807 Space Plasma Physics: Charged particle motion and acceleration; 2164 Interplanetary Physics: Solar wind plasma; 7511 Solar Physics, Astrophysics, and Astronomy: Coronal holes; *KEYWORDS:* ion-cyclotron instability, ion drift, thermal anisotropy, qlm cascade

Citation: Gomberoff, L., and J. A. Valdivia, Ion cyclotron instability due to the thermal anisotropy of drifting ion species, *J. Geophys. Res.*, *108*(A1), 1050, doi:10.1029/2002JA009576, 2003.

1. Introduction

[2] It is generally believed that heating and acceleration of heavy ions in the lower corona is due to resonant absorption of Alfvén waves [see, e.g., *Gomberoff et al.*, 1996; *Marsch*, 1998; *Tu and Marsch*, 1999; *Hu and Habbal*, 1999; *Cranmer et al.*, 1999a, 1999b; *Cranmer*, 2000; *Isenberg and Hollweg*, 1983]. However, low-frequency Alfvén waves (0.001–0.1Hz) which dominate the power spectrum of magnetic fluctuations in the solar wind for distances larger than 0.3 AU, are not likely to heat and accelerate the heavy ions to the observed values. On the other hand, high-frequency Alfvén waves ($10-10^4$ Hz) that might be responsible for ion cyclotron heating and acceleration of these ions, have not yet been observed either in the solar wind or in the corona [*Cranmer et al.*, 1999a, 1999b]. However, there are several proposals as to how these waves might be generated. Thus, it has been suggested that high-frequency Alfvén waves can be generated by a turbulent cascade [see, e.g., *Tu and Marsch*, 1995]. It has also been suggested that high-frequency Alfvén waves can be generated by microflares that are then converted to ion cyclotron waves at higher coronal altitudes [*Axford and Mckenzie*, 1992, 1996].

[3] Not only high-frequency waves have not been observed, but there are other problems with ion cyclotron heating, such as, the observations on the preferential heating of O^{+5} [*Kohl et al.*, 1998, 1999a, 1999b] which are not satisfactorily explained by this mechanism[*Tu and Marsch*, 2001]. There are also other approaches to this problem. These include fast and oblique propagation of ion cyclotron waves [*Leamon et al.*, 2001; *Li and Habbal*, 2001; *Markovskii*, 2001; *Hollweg and Markovskii*, 2002], the need to develop a kinetic treatment [*Isenberg et al.*, 2001; *Isenberg*, 2001], fastshock heating [*Lee and Wu*, 2000; *Lee*, 2001], turbulence-driven ion cyclotron waves [*Li et al.*, 1999], and others. Nevertheless, there seems to be some observational evidence that parallel propagating ion cyclotron waves are at the origin of ion heating and acceleration [*Tu and Marsch*, 2001; *Isenberg et al.*, 2001; *Isenberg*, 2001].

[4] Observations of heating and acceleration of heavy ions in the solar corona by SOHO, have shown very large thermal anisotropy for O^{+5} ions with values ranging between $10 < T_\perp/T_\| < 100$ [*Kohl et al.*, 1998, 1999a, 1999b; *Li et al.*, 1998; *Cranmer et al.*, 1999a, 1999b]. In a previous paper [*Gomberoff and Valdivia*, 2003], it was suggested that the heavy ion drift velocity relative to the

0148-0227/03/2002JA009576

protons, and large thermal anisotropy can trigger a cascade of ion cyclotron waves to much higher frequencies. These waves would then be absorbed by ion species having larger charge to mass ratio. Ion cyclotron waves due to heavy ion thermal anisotropy have also been considered by *Gary et al.* [2001] and *Ofman et al.* [2001]. However, these authors did not include the important effect of heavy ion drift velocity [see *Gomberoff and Valdivia*, 2003].

[5] Here we continue to develop this idea by including anisotropic alpha particles into the problem. It is shown that due to the much larger density of the alpha particles relative to oxygen ions in the solar wind, a much smaller thermal anisotropy is required to trigger large growth rates of the proton-cyclotron instability [see *Gomberoff and Valdivia*, 2003]. The observation that a species drift velocity and thermal anisotropy can lead to an instability beyond the species gyrofrequency, provides a complementary ion heating and acceleration mechanism in the solar corona.

[6] We also analyze the very complex situation in which the unstable spectrum is produced by two thermally anisotropic heavy ion components. The combined effect of two heavy ion components can trigger very strong ion cyclotron waves above their corresponding gyrofrequency, and the minor ions can also contribute to enhance the proton-cyclotron instability produced by just one species [*Gomberoff and Valdivia*, 2003].

[7] The paper is organized as follows. In section 2, we derive the general ion cyclotron dispersion relation for any number of drifting heavy ion species using the semicold approximation. In section 3 we derive and discuss the particular case when the heavy ion species are drifting alpha particles. In section 4,we discuss the case of two drifting ion components: O^{+6} and alpha particles. In section 5, the results are summarized.

2. Ion Cyclotron Dispersion Relation

[8] We consider a plasma in an external magnetic field B_0, composed of electrons, protons, and a number of heavy ion species drifting relative to the protons, along the external magnetic field. The j^{th} minor heavy ion species has normalized velocities, $U_j = V_j/V_A$, where V_j is the heavy ion velocity normalized to the Alfvén velocity, $V_A = B_0/\sqrt{(4\pi n_p m_p)}$, with n_p as the proton density and m_p as the proton mass. The dispersion relation for ion cyclotron waves moving in the direction of the external magnetic field, assuming bi-Maxwellian distribution functions, is [see, e.g., *Gomberoff*, 1992],

$$y^2 \sum_j \left\{ \frac{z_j \eta_j A_j}{M_j} - z_j \eta_j (x - yU_j) - \frac{z_j \eta_j}{M_j^2 y \beta_{\|j}^{1/2}} Z(\xi_j) G_j \right\}, \quad (1)$$

$$G_j = \left[A_j \left(1 - M_j (x - yU_j)\right) - M_j (x - yU_j) \right], \quad (2)$$

where the sum is over all ion species, including the proton background. In equation (1), $x = \omega/\Omega_p$, $y = kV_A/\Omega_p$, $n_j = n_j/n_p$, $A_j = T_{\perp j}/T_{\|j} - 1$ is the ion thermal anisotropy, $M_j = m_j/z_j m_p$ (with m_j the ion mass and z_j the degree of ionization of the heavy ion), Z is the plasma dispersion function [*Fried and Conte*, 1961], $\xi_j = (M_j(x - yU_j) - 1)/M_j y \beta_{\|j}^{1/2}$, $\beta_{\|j} = v_{\mathrm{th},j}^2/V_A^2$ where $v_{th,j}^2 = 2KT_j/m_j$ is the thermal velocity of ion components, and K is the Boltzmann constant. In this equation we have assumed a current-free system, and the bulk protons has been chosen to be the rest frame [*Gomberoff and Valdiva*, 1991]. We shall assume all betas to be much smaller than 1, so that we can use the semicold approximation [see, e.g., *Gomberoff*, 1992]. Thus, using the large argument expansion of the Z-functions, and assuming ω to be complex, we obtain from the real part of equation (1) the cold plasma dispersion relation,

$$y^2 = \sum_j \frac{z_j M_j \eta_j (x - yU_j)^2}{1 - M_j (x - yU_j)}, \quad (3)$$

On the other hand, assuming $|Re(\xi_j)| \gg |Im(\xi_j)|$, from the imaginary part of equation (1) we obtain the growth/damping rate,

$$\gamma = \sum_j \frac{\sqrt{(\pi)} z_j \eta_j}{M_j^2 y \beta_{\|j}^{1/2}} \frac{G_j}{F(x,y)} exp\left[- \left(\frac{1 - M_j (x - yU_j)}{M_i y \beta_{\|j}^{1/2}} \right)^2 \right] \quad (4)$$

where

$$F(x,y) = \sum_j \frac{z_j M_j \eta_j (x - yU_j)\left(2 - M_j (x - yU_j)\right)}{\left(1 - M_j (x - yU_j)\right)^2}. \quad (5)$$

[9] The sign of the growth (or dissipation) rate is controlled by G, equation (2), and for the case of the proton background it yields, $G_p = A_p(1 - x) - x$. If the proton background has no thermal anisotropy, then the protons contribute with pure absorption. On the other hand, if $A_p > 0$ it will lead to instability for $x < A_p/(A_p + 1)$ [see, e.g., *Gomberoff and Neira*, 1983; *Gomberoff and Vega*, 1987; *Gomberoff and Elgueta*, 1991]. Even though these considerations may affect the total growth rate in situations of interest, we shall take $A_p = 0$ for the rest of the paper in order to simplify the problem. Similarly, if the ion drift velocity is $U_j = 0$, then the instability occurs always below the gyrofrequency of the anisotropic specie.

3. Alpha Particles

[10] As pointed out in the introduction, in a previous paper [*Gomberoff and Valdivia*, 2003], we studied the effect of drifting O^{+6} ions on the ion cyclotron instability triggered by the thermal anisotropy of oxygen ions. It was shown that due to the oxygen drift velocity and large thermal anisotropy, proton-cyclotron waves can be generated. Since this effect depends on the species thermal anisotropy and branching ratio, the maximum growth rate for O^{+6} was less than 10^{-3} for a thermal anisotropy of $A_{O+6} = 100$. Here we shall study the same effect, but for alpha particles that are much more abundant than oxygen ions. Therefore, we expect that much smaller alpha particle thermal anisotropy is required to trigger proton-cyclotron waves.

[11] Thus, for the particular case of stationary protons and drifting alpha particles equations (2) and (3) yield,

$$y^2 = \frac{x^2}{1 - x} + \frac{4\eta_\alpha (x - yU_\alpha)^2}{1 - 2(x - yU_\alpha)}, \quad (6)$$

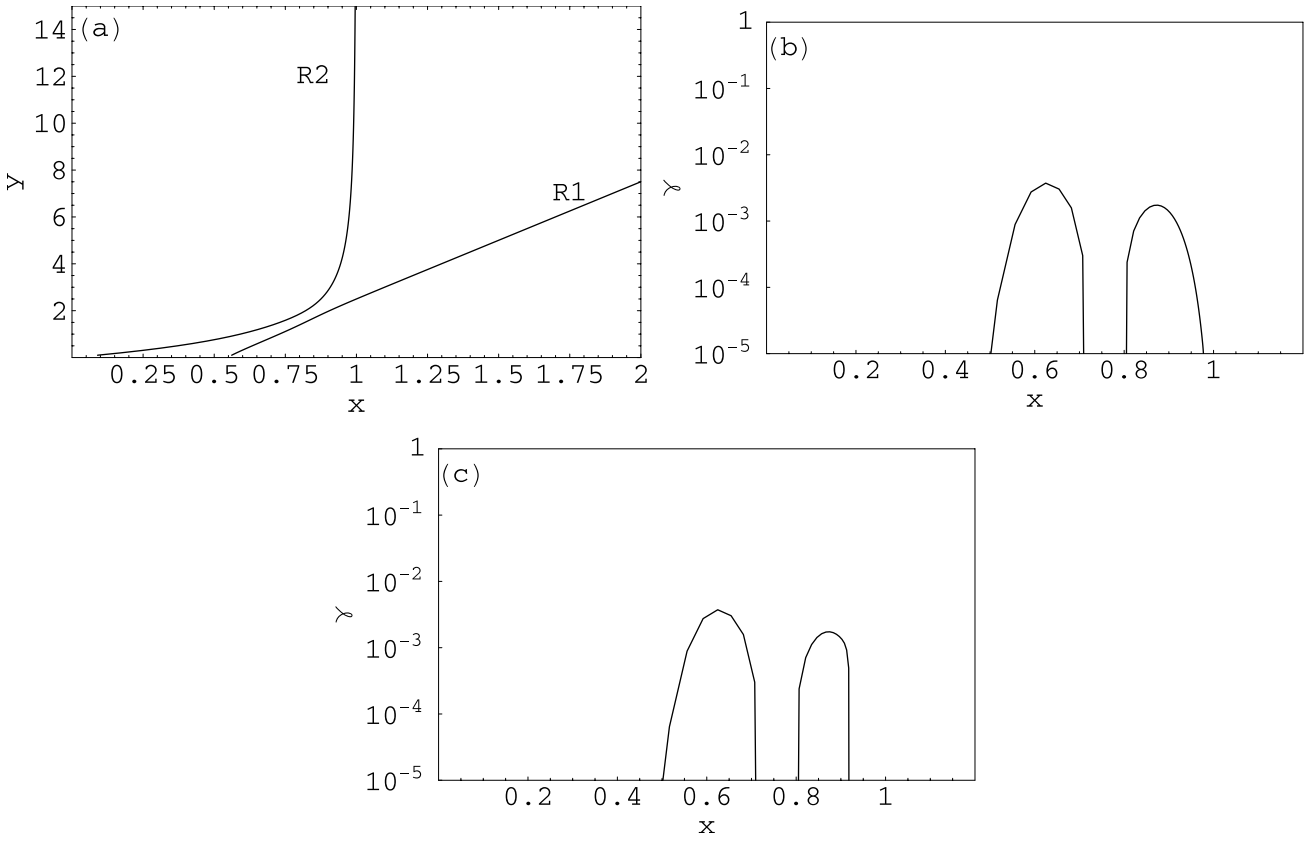

Figure 1. (a) Dispersion relation equation (6), $y = kV_A/\Omega_p$ versus $x = \omega/\Omega_p$, for $\eta_\alpha = 0.05$, $U_\alpha = 0.2$. The two relevant roots are marked as (R1) and (R2) respectively. (b) Corresponding growth rate for (R2), equation (7), for $\beta_{\|\alpha} = 0.004$, $A_\alpha = 6$, and $\beta_{\|p} = 10^{-6}$. (c) The same as (b), but for $\beta_{\|p} = 10^{-4}$.

and

$$\gamma_{p,\alpha} = \frac{\sqrt{(\pi)}\eta_\alpha}{2y\beta_{\|\alpha}^{1/2}}\frac{G_\alpha}{F(x,y)} exp\left[-\left(\frac{1-2(x-yU_\alpha)}{2y\beta_{\|\alpha}^{1/2}}\right)^2\right] - \frac{\sqrt{(\pi)}x}{y\beta_{\|p}^{1/2}}\frac{1}{F(x,y)} exp\left[-\left(\frac{1-x}{y\beta_{\|p}^{1/2}}\right)^2\right], \quad (7)$$

with

$$G_\alpha = A_\alpha(1-2(x-yU_\alpha)) - 2(x-yU_\alpha),$$

and

$$F(x,y) = \frac{(2-x)x}{(1-x)^2} + \frac{8\eta_\alpha(1-(x-yU_\alpha))(x-yU_\alpha)}{(1-2(x-yU_\alpha))^2}.$$

[12] As it is well known, when there is no drift velocity between the ion species the dispersion relation has two branches each going asymptotically to the corresponding gyrofrequency [see, e.g., *Gomberoff and Neira*, 1983; *Gomberoff and Elgueta*, 1991]. In this case, the instability occurs for frequencies below the thermally anisotropic species gyrofrequency.

[13] On the other hand, when the ion species are drifting relative to each other, the situation is different. In Figure 1a we show the dispersion relation equation (6) for $\eta_\alpha = 0.05$ and $U_\alpha = 0.2$. The upper curve of the dispersion relation corresponds to the proton branch (R2), and the other to the drifting alpha particles (R1). Note that the latter satisfies $x - yU_\alpha \simeq 0.5$. In Figure 1b we display the corresponding growth rate, equation (7), for $A_\alpha = 6$, $\beta_{\|\alpha} = 0.004$ and $\beta_{\|p} = 10^{-6}$. As it follows from Figure 1b, the maximum proton-cyclotron growth rate is now larger than 10^{-3} for an alpha particle thermal anisotropy of only $A_\alpha = 6$ [see *Gomberoff and Valdivia*, 2003]. The value $\beta_p = 10^{-6}$ used in Figure 1b is unrealistic at the base of the solar corona, because it would imply a relativistic Alfven velocity. For this reason in Figure 1c we have increased β_p by two orders of magnitude to $\beta_p = 10^{-4}$, which is a plausible value of β_p in this region. Due to the larger proton absorption rate, there is a decrease of the high-frequency instability range. It is important to emphasize that both instability regions are solutions of the branch of the dispersion relation which goes asymptotically to the proton gyrofrequency (R2).

[14] In order to study the dependence of γ_{max} for the branch of the growth rate closer to the proton gyrofrequency (see Figures 1b and 1c), we have constructed a three-dimensional plot of γ_{max} versus U_α and $\beta_{\|\alpha}$ (Figure 2a) and γ_{max}

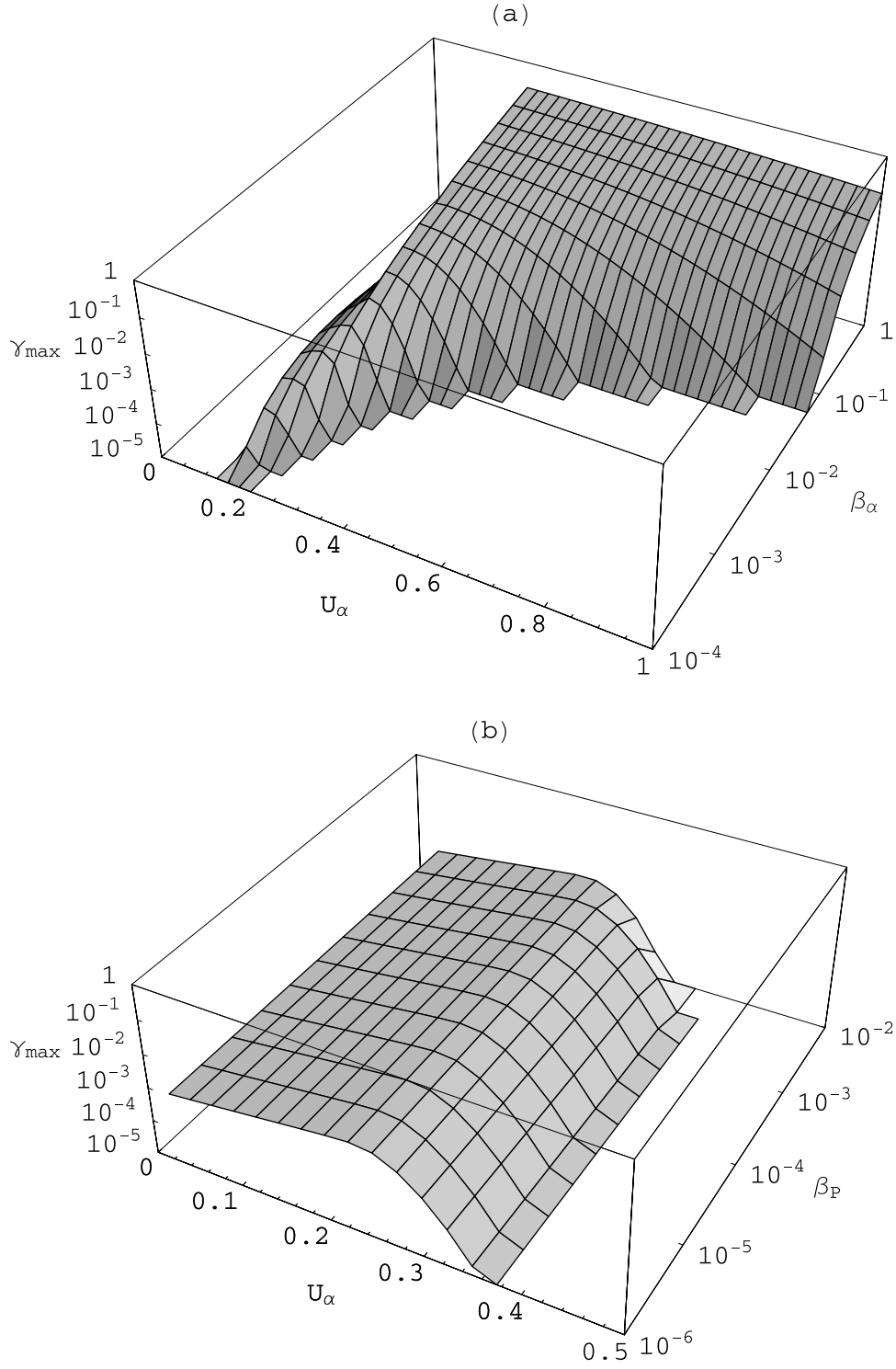

Figure 2. (a) Three-dimensional plot of γ_{max} versus U_α and $\beta_{\|\alpha}$ for the (R2) root, using $\beta_{\|p} = 10^{-6}$. (b) Three-dimensional plot of γ_{max} versus U_α and $\beta_{\|p}$ for the (R2) root, using $\beta_{\|\alpha} = 0.004$. We take $A_\alpha = 6$.

versus U_α and $\beta_{\|p}$ (Figure 2b) for $A_\alpha = 6$. As expected, as we increase $\beta_{\|p}$ the ion cyclotron waves are strongly affected by the proton absorption. The maximum growth rate of the ion cyclotron waves depends strongly on the alpha's drift velocity, as shown in Figure 3 at multiple cross-sections of Figure 2a for fixed $\beta_{\|\alpha} = 0.001$, 0.005,0.01, as indicated in the corresponding figures.

[15] The $\beta_{\|p}$ of the protons will be chosen very small to illustrate that the high-frequency waves, close the proton gyrofrequency, can indeed be generated by the thermal anisotropy of the drifting minor ions. For Oxygen ions it has been shown by *Gomberoff and Valdivia* [2003], that as we increase $\beta_{\|p}$ the growth rate of the waves is partially reduced suggesting that the protons are

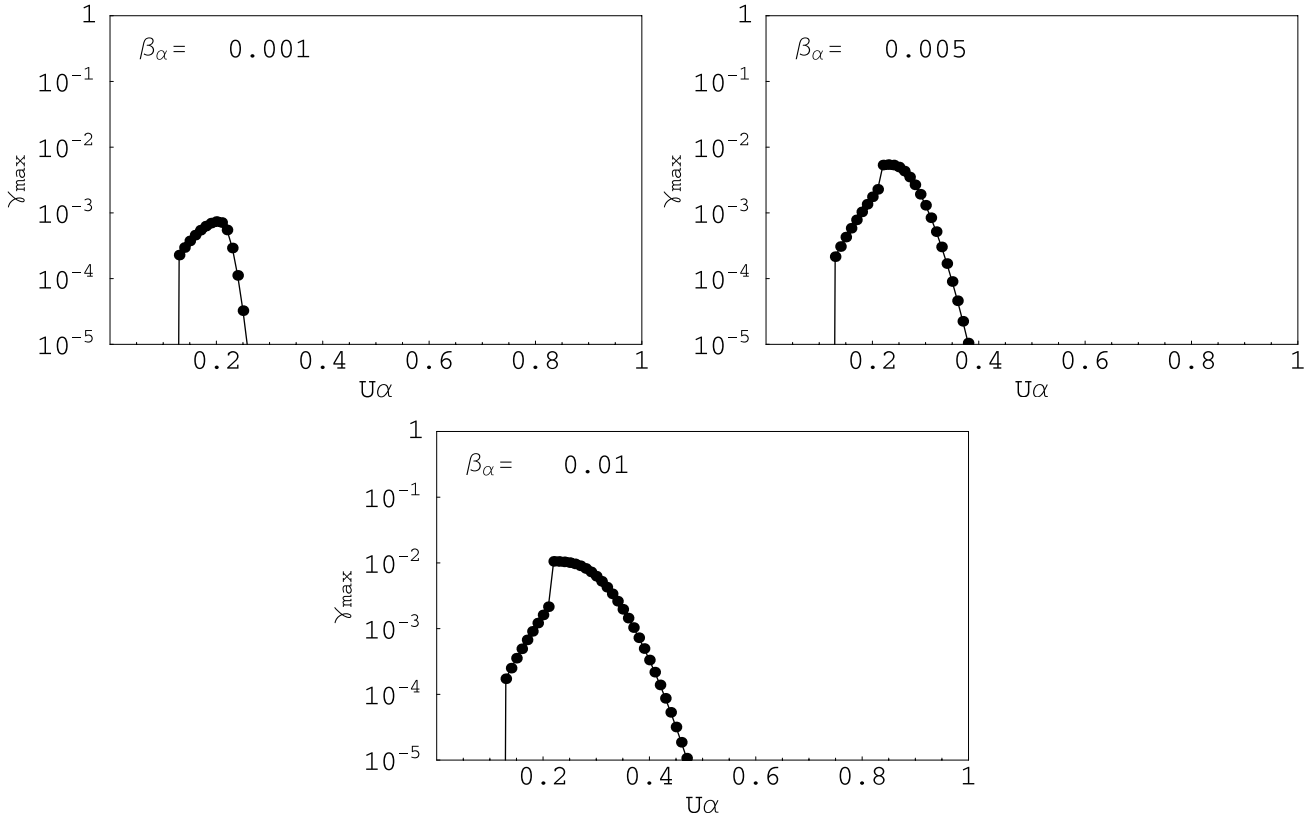

Figure 3. Cross-sections of Figure 2a for several values of $\beta_{\|\alpha} = 0.001, 0.005, 0.01$.

capable to absorbing these waves. In this paper we are concerned with characterizing the parameters controlling the generation of the high-frequency proton-cyclotron waves in the initial stages, and for that $\beta_{\|p} = 10^{-6}$ has been chosen very small in order to emphasize this effect. Moreover, an exact calculation of equation (1) (to be published elsewhere) shows that the semicold approximation gives much too large proton absorption rates close to $\omega \simeq \Omega_p$. This is to be expected because as $\beta_{\|p}$ increases, the semicold approximation breaks down for ω close to Ω_p. However, for the purpose of the present paper, the semicold approximation is perfectly appropriate. After this linear regime, the evolution of the energy transfer between ions must be described in a nonlinear fashion, which requires a different approach that will be published elsewhere.

[16] We shall now show that the lower branch of the dispersion relation—the one satisfying $x - yU_\alpha \simeq 1/2$ (see R1 in Figure 1a)—can also become unstable, but for rather large values of the alpha thermal anisotropy, A_α. In order to illustrate this result, in Figure 4a we have plotted γ versus frequency for $A_\alpha = 500$, $\beta_{\|\alpha} = \beta_{\|p} = 10^{-6}$, and $U_\alpha = 0.6$. From this figure it follows that, for these conditions, the spectrum has a double hump and is very broad. As the drift velocity goes down, the double humped spectrum shows now a single peak. This effect is illustrated in Figure 4b for $U_\alpha = 0.45$, and in Figure 4c for $U_\alpha = 0.24$. In Figure 5a we have plotted γ_{max} for $x > 1$, as a function of A_α and $\beta_{\|\alpha}$ for fixed $U_\alpha = 0.5$ and $\beta_{\|p} = 10^{-6}$. As expected, there is a sharp increase of γ_{max} with $A_\alpha \simeq 200$. In Figure 5b we have done the same as in Figure 5a, but for γ_{max} as a function of A_α and U_α, for fixed $\beta_{\|p} = \beta_{\|\alpha} = 10^{-6}$. Here we see an interesting interplay between the alpha's drift velocity and its thermal anisotropy, as it is illustrated in the cross-sections of Figure 6, for several values of $U_\alpha = 0.2, 0.3, 0.4, 0.6, 0.8$, which are indicated in the corresponding figure.

4. Alpha Particles and Oxygen Ions

[17] In *Gomberoff and Valdivia* [2003], it was contended that since we are dealing with a linear theory, the combined effect of many heavy ion species could lead to an important growth rate of the proton-cyclotron instability. To study this situation, we add to the model an additional highly anisotropic component, O^{+6}. We note that observations show a large thermal anisotropy for O^{+5} ions [*Kohl et al.*, 1998; *Li et al.*, 1998; *Kohl et al.*, 1999a, 1999b]. However, we assume a large thermal anisotropy for O^{+6} as well, because its branching ratio is much larger than that of O^{+5} ions [see *Gomberoff and Valdivia*, 2003].

[18] The corresponding dispersion relation and growth rate are given by,

$$y^2 = \frac{x^2}{1-x} + \frac{4\eta_\alpha (x - yU_\alpha)^2}{1 - 2(x - yU_\alpha)} + \frac{16\eta_{O^{+6}} (x - yU_{O^{+6}})^2}{1 - \frac{16}{6}(x - yU_{O^{+6}})}, \qquad (8)$$

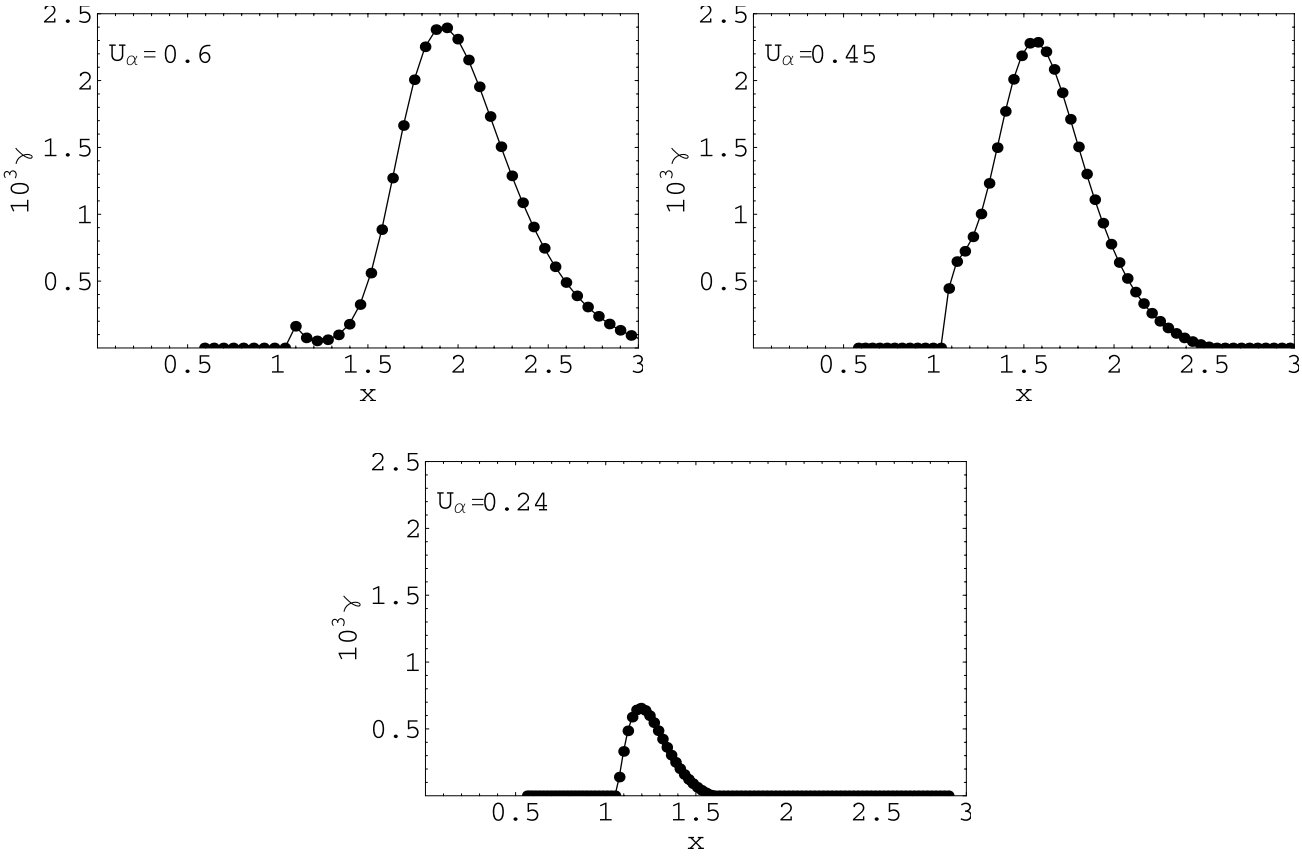

Figure 4. (a) Growth rate γ versus normalized frequency, x, for $A_\alpha = 500$, $\beta_{\|\alpha} = \beta_{\|p} = 10^{-6}$, and $U_\alpha = 0.6$. (b) Same as (a), but for $U_\alpha = 0.45$. (c) Same as (a), but for $U_\alpha = 0.24$.

and

$$\gamma = \gamma_{p,\alpha}\frac{F(x,y)}{\bar{F}(x,y)} + \frac{6\sqrt{(\pi)}\eta_{O^{+6}}}{\left(\frac{16}{6}\right)^2 y\beta_{\|O^{+6}}^{1/2}}\frac{G_{O^{+6}}}{\bar{F}(x,y)}exp\left[-\left(\frac{1-\left(\frac{16}{6}\right)(x-yU_{O^{+6}})}{\left(\frac{16}{6}\right)y\beta_{O^{+6}}^{1/2}}\right)^2\right], \quad (9)$$

with

$$G_{O^{+6}} = A_{O^{+6}}\left(1-\left(\frac{16}{6}\right)(x-yU_{O^{+6}})\right) - \left(\frac{16}{6}\right)(x-yU_{O^{+6}})$$

and

$$\bar{F}(x,y) = F(x,y) + \frac{16\eta_{O^{+6}}(x-yU_{O^{+6}})\left(2-\left(\frac{16}{6}\right)(x-yU_{O^{+6}})\right)}{\left(1-\left(\frac{16}{6}\right)(x-yU_{O^{+6}})\right)^2).}$$

[19] In the case when there is more than one heavy ion specie, the situation is, of course, more complicated. Since there are many parameters involved, a systematic analysis is difficult. In the following we shall illustrate the main features.

[20] To this end, in Figure 7a we begin by plotting the dispersion relation, equation (8), when the drift velocity of the heavy ions is zero relative to the protons. In Figure 7b we show the corresponding growth rates, equation (9), for $A_{O^{+6}} = 100$, $A_\alpha = 6$, $\beta_\alpha = 0.005$, $\beta_{O^{+6}} = 0.0004$, and a very low $\beta_p = 10^{-6}$. A very small $\beta_{\|p}$ has been used in order to illustrate the results by diminishing proton absorption effects. The first peak is due to the O^{+6} ions, i.e., the dispersion curve denoted by the dotted line (R3) in Figure 7a. The second peak corresponds to the alpha particles, and has been denoted by the solid line (R2) in Figure 7a.

[21] In the following figures, we vary the drift velocities of the heavy species without changing the other parameters.

[22] Thus in Figure 8a we show the instability regions for $U_\alpha = 0.2$, and $U_{O^{+6}} = 0$. The roots are denoted by (R1), (R2), (R3), and (R4), but only the first three belong to the region of interest. The unstable roots of Figure 8a correspond to (R2), solid line, and (R3), dotted line, as indicated there. The (R2) root is clearly double humped, while the (R3) root is single humped. Figure 8a is similar to Figure 1b, but with another peak due to O^{+6}. As $U_{O^{+6}}$ increases there is a large increase of the high-frequency band of the (R3) root as shown in Figures 8b and 8c for $U_{O^{+6}} = 0.1$ and $U_{O^{+6}} = 0.15$, respectively. From Figures 8b and 8c one can clearly see how the O^{+6} ions start generating the ion cyclotron waves. The effect of this branch (R3) is due to oxygen thermal anisotropy and corresponds to Figure 2b of *Gomberoff and Valdivia* [2003]. The dispersion relation shown in Figure 8d, for $U_\alpha = 0.2$ and $U_{O^{+6}} = 0.1$, suggests a complicated interplay among its different branches.

[23] In Figure 9a we have taken $U_{O^{+6}} = U_\alpha = 0.2$, and in Figure 9b we have increased $U_{O^{+6}} = 0.25$. The effect of

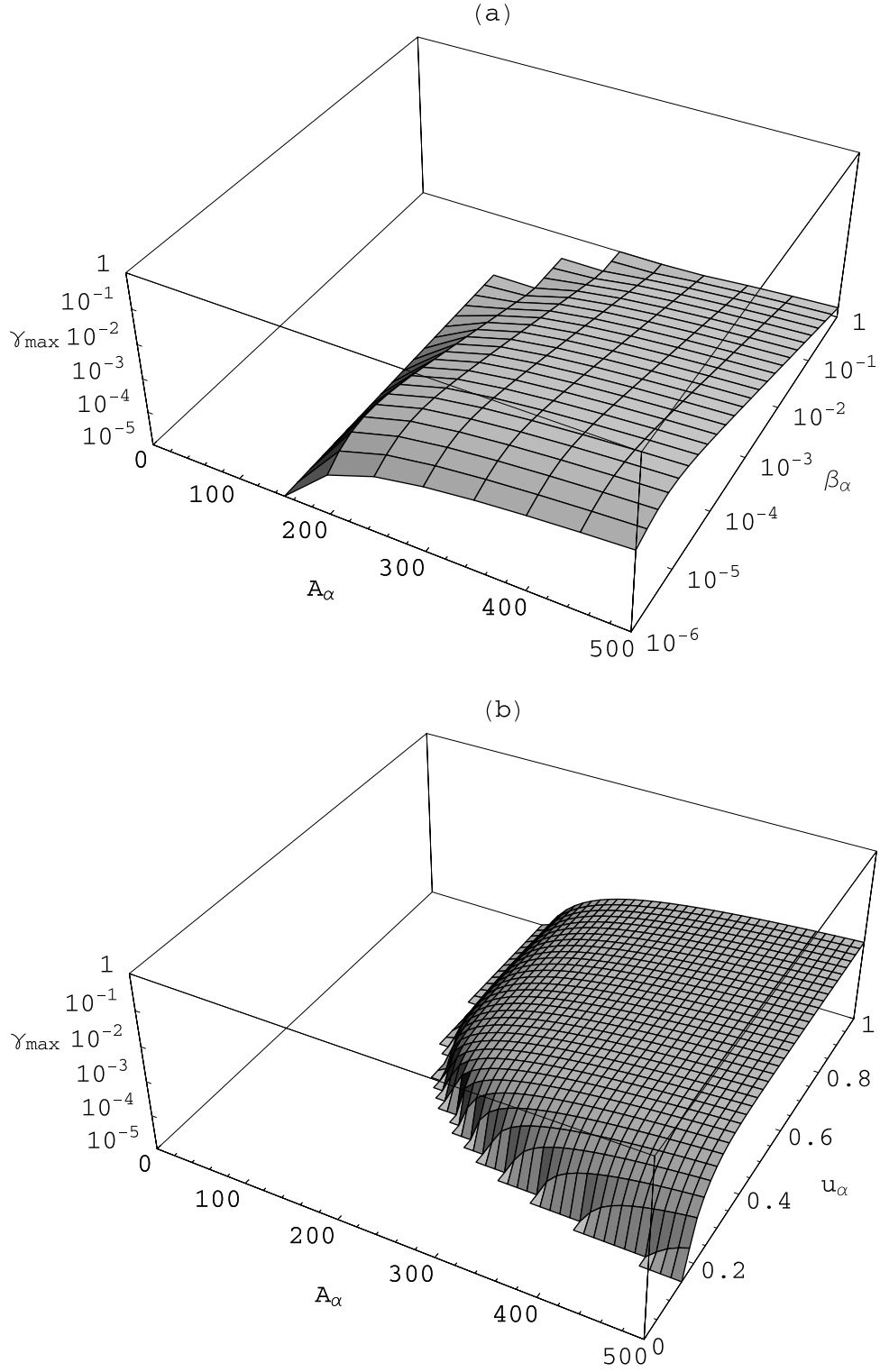

Figure 5. (a) Three-dimensional plot of γ_{max} versus A_α and $\beta_{\|\alpha}$ using $\beta_{\|p} = 10^{-6}$ and $U_\alpha = 0.5$. (b) Three-dimensional plot of γ_{max} versus A_α and U_α using $\beta_{\|p} = \beta_{\|\alpha} = 10^{-6}$.

increasing the drift velocity of O^{+6} beyond U_α is to stabilize the waves. The waves generated by the root (R2), solid line, are completely dissipated and only the (R3) root, dotted line, survives.

[24] In Figure 10a, we illustrate the behavior of γ_{max} for the (R2) root, as a function of varying $U_{O^{+6}}$ for fixed $U_\alpha = 0.2$. In Figure 10a we do the same as in Figure 10a, but for $U_\alpha = 0.3$. From Figure 10 one can clearly see the stabilization of the (R3) root of the system for $U_{O+6} \geq U_\alpha$.

[25] Finally, in Figure 11, we illustrate the effect of increasing U_α while keeping $U_{O^{+6}} = 0.2$ fixed. Thus, in

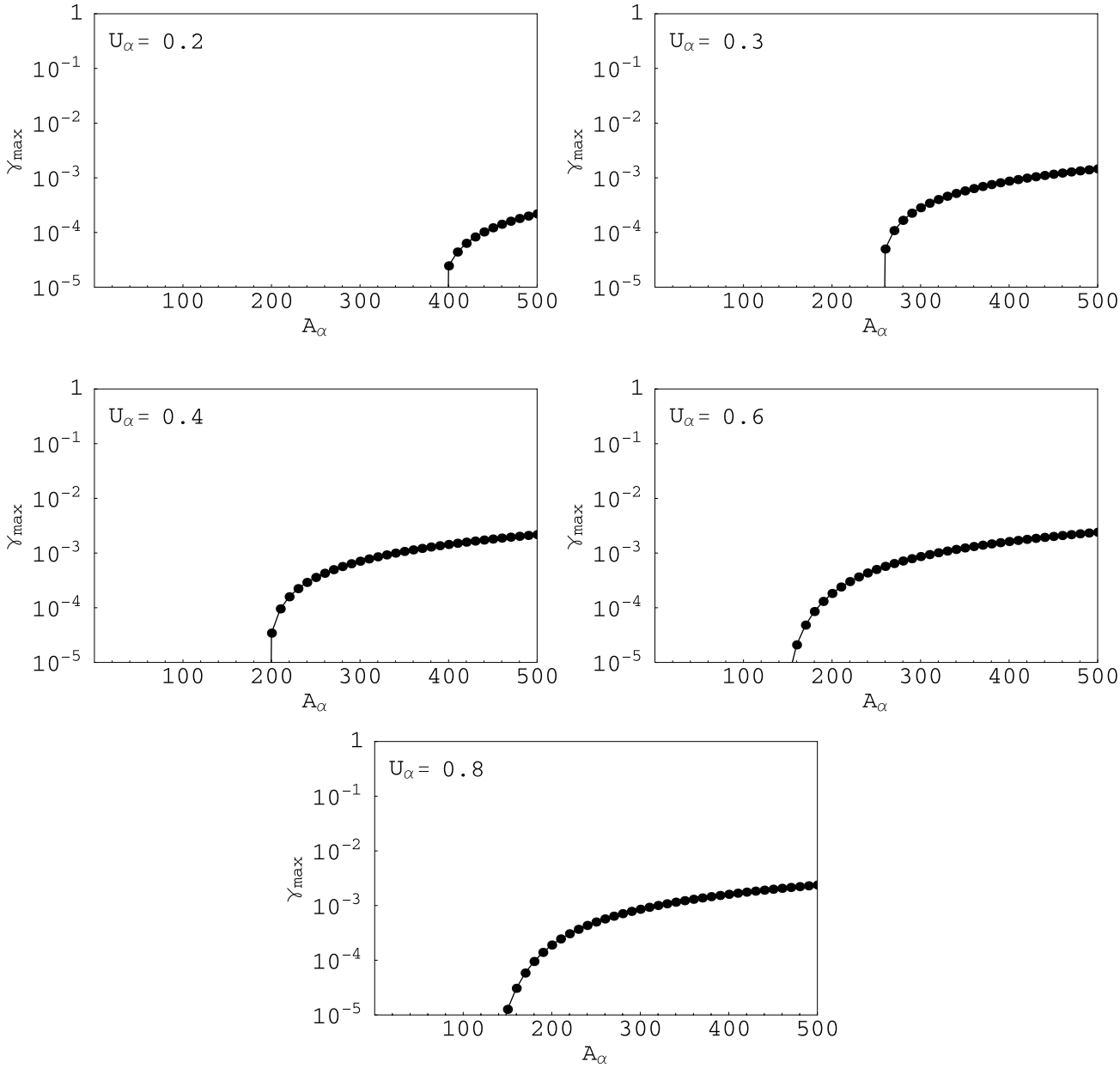

Figure 6. Cross-sections of Figure 5b for several values of U_α = 0.2, 0.3, 0.4, 0.6, 0.8.

Figures 11a–11d we have taken U_α = 0.1, 0.15, 0.18, 0.19 respectively. The unstable roots correspond to (R3), dotted line, in Figures 11a and 11b, and to (R3) and (R2), solid line, in Figures 11c and 11d. In Figure 11c the unstable root corresponding to (R2) does not appear, because $\gamma < 10^{-5}$. As it follows from Figure 11a, the effect of increasing the drift velocity of the alpha particles is to stabilize the high-frequency branch of the spectrum. However, if U_α is further increased to $U_\alpha = 0.15$, the high-frequency branch reappears as shown in Figure 11b. In Figure 11c we have raised U_α = 0.18. As a consequence, there is a large increase in the maximum growth rate of the high-frequency branch, and also another root becomes unstable (R2). In Figure 11d, U_α has been raised a little further to U_α = 0.19, and a new instability branch appears in between the two larger peaks of the previous figure. This new instability also corresponds to the root denoted by (R2).

5. Summary

[26] We have continued the study of the combined effect of heavy ion thermal anisotropy and drifting velocity on the ion cyclotron instability. This study was initiated by *Gomberoff and Valdivia* [2003], in an attempt to explain the proton heating observed at the base of solar coronal holes, by making use of the large oxygen ion thermal anisotropy observed there [*Kohl et al.*, 1998, 1999a, 1999b; *Cranmer*, 2000].

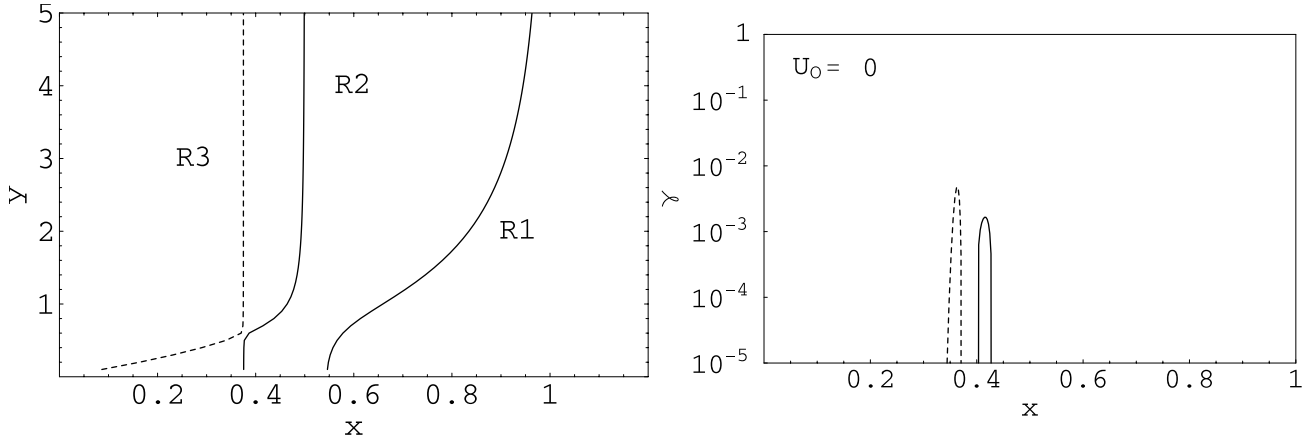

Figure 7. (a) Dispersion relation, equation (8), y versus x for $\eta_{O^{+6}} = 0.0002$, $\eta_\alpha = 0.05$ for $U_{O^{+6}} = U_\alpha = 0$. The roots are denoted by (R1), (R2), (R3) and (R4), but only the first three belong to the region of interest. (b) Corresponding growth rates, equation (9), versus x for $A_{O^{+6}} = 100$, $A_\alpha = 6$, $\beta_{\|O^{+6}} = 0.0004$ $\beta_{\|\alpha} = 0.005$, and $\beta_{\|p} = 10^{-6}$. The unstable roots are (R2), solid line, and (R3), dotted line.

[27] To this end, we have first considered the effect of alpha particles thermal anisotropy and drift velocity on the ion cyclotron instability. It is shown that as compared to oxygen ions, a much smaller thermal anisotropy is required to trigger a much larger proton-cyclotron instability growth rate. This effect is illustrated in Figures 1b and 1c. A three-dimensional study of the maximum growth rate, including the simultaneous effects of drift velocity U_α, and $\beta_{\|\alpha}$, is shown in Figure 2. The unstable branch of the dispersion relation corresponds to the upper branch of Figure 1a, denoted by R2.

[28] We have also shown that the lower branch of the dispersion relation, R1, can become unstable for frequencies beyond the proton gyrofrequency. This occurs for large

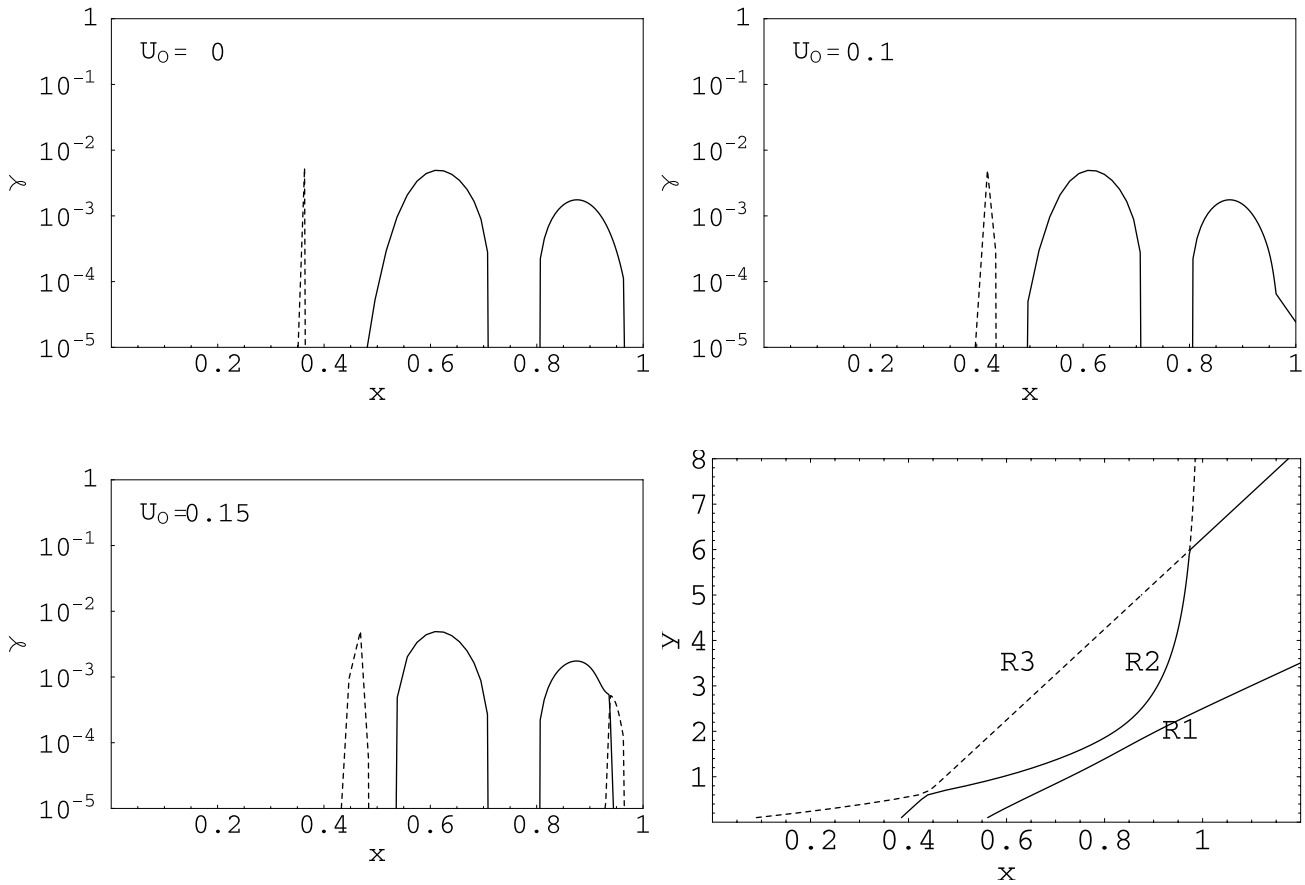

Figure 8. Growth rate versus x for the case of Figure 7, but for $U_\alpha = 0.2$ and (a) $U_{O^{+6}} = 0.0$, (b) $U_{O^{+6}} = 0.1$,(c) $U_{O^{+6}} = 0.15$. The unstable roots are (R2), solid line, and (R3), dotted line. (d)The dispersion relation for the case $U_{O^{+6}} = 0.1$.

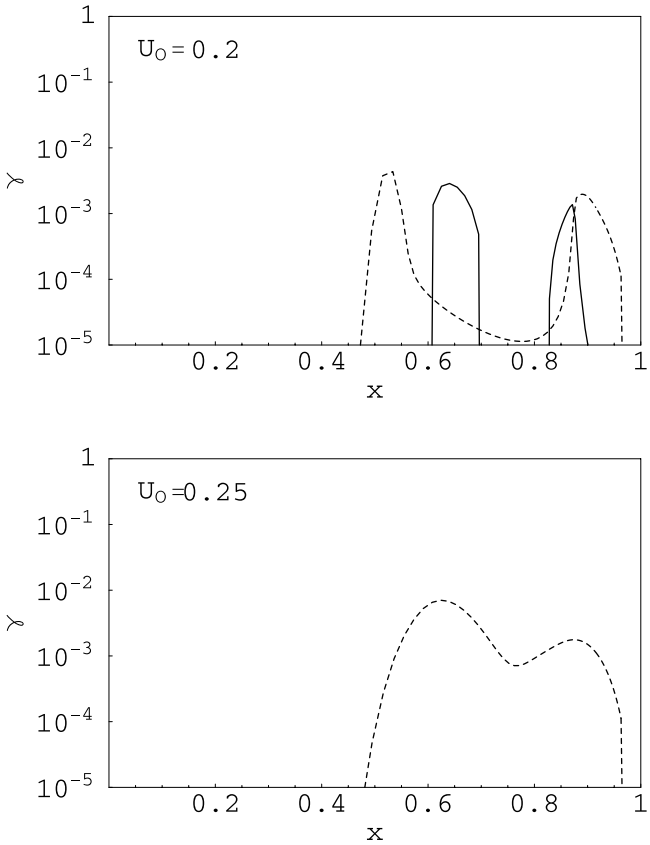

Figure 9. (a) Same as Figure 8, but for $U_{O^{+6}} = 0.2$. (b) Same as (a) but for $U_{O^{+6}} = 0.25$. The unstable roots are (R2), solid line, and (R3), dotted line.

values of the alpha particle thermal anisotropy, and very low values of $\beta_{\|\alpha}$. These results are illustrated in Figure 4.

[29] Finally, we have studied the combined effect of oxygen ions and alpha particles. Since there are several parameters involved, a systematic analysis is difficult. In an attempt to do this, we have done the following. We have started with a situation corresponding to the three species at rest relative to each other. In this case, as it is well known, there are two unstable branches below the corresponding gyrofrequencies. The corresponding marginal modes are given by $x_{m,j} = (\Omega_j/\Omega_p)(A_j/(A_j + 1)$, with $j = O^{+5}$, α [see, e.g., *Gomberoff and Valdivia*, 2003]. This is shown in Figure 7b. We have then increased the $U_{O^{+6}}$ drift velocity. As it is expected, a new branch appears close to the proton gyrofrequency. Then, in Figure 8 we have considered several values of $U_{O^{+6}}$ while keeping $U_\alpha = 0.2$ fixed. The system shows a complicated interplay among the branches of the dispersion relation. Both the (R2) and (R3) roots are now unstable. The effect of increasing the O^{+6} drift velocity beyond the α-particle drift velocity is to stabilize the waves belonging to the (R2) root. Finally, in Figure 11 we illustrate the behavior of the growth rate for varying U_α while keeping $U_{O^{+6}} = 0.2$ fixed. In this case the unstable root is (R3) in Figures 11a and 11b, and (R3) and (R2) in Figures 11c and 11d.

[30] As pointed out above, a systematic study that would allow for an exact prediction of the effect of changing the various parameters involved, is difficult. However, one can conclude that, in general, heavy ion thermal anisotropy and drift velocity (relative to the protons) can trigger ion cyclotron waves above their corresponding gyrofrequency leading, thereby, to resonant effects with ion species having larger charge to mass ratios. Also, the combined effect due to several heavy ion components can lead to a large enhancement of the ion cyclotron instability, both for low and high frequencies. Due to ion cyclotron interaction heavy ions become anisotropic.

[31] Since high-frequency ion cyclotron waves are not observed at the base of the corona nor in the fast solar wind, the results of this paper naturally suggest a possible cascade mechanism that utilizes low-frequency ion cyclotron waves in the coronal holes to heat anisotropically larger and larger q/m ions. First, low-frequency ion cyclotron waves can heat anisotropically ion components with small q/m ratio. This anisotropy, complemented with the ion drift velocity, can generate instabilities for larger frequencies, which in turn can heat anisotropically ions of larger q/m ratio. Once these last ions are anisotropically heated, they can generate instabilities of even larger frequencies, in a process that may repeat until it reaches the protons. This is the phenomenon that we denominate a "cascade mechanism", and of course we do not pretend that this is the unique phenomenon responsible for the observations, but it may provide a possible contribution. However, at larger heliocentric distances

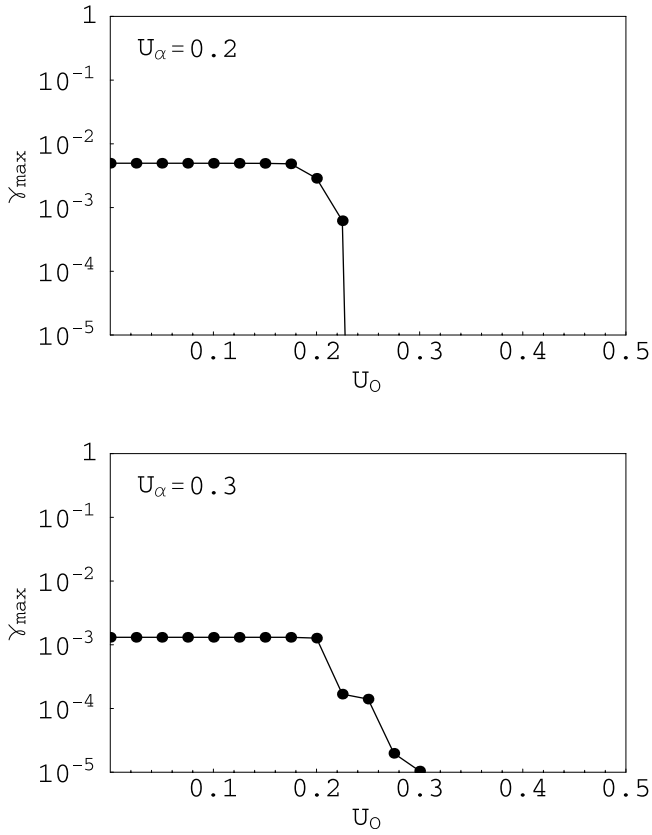

Figure 10. (a) The maximum growth rate γ_{max} as a function of $U_{O^{+6}}$ for the same parameters as in Figure 9, but for $U_\alpha = 0.2$. The same as in (a) but for $U_\alpha = 0.3$.

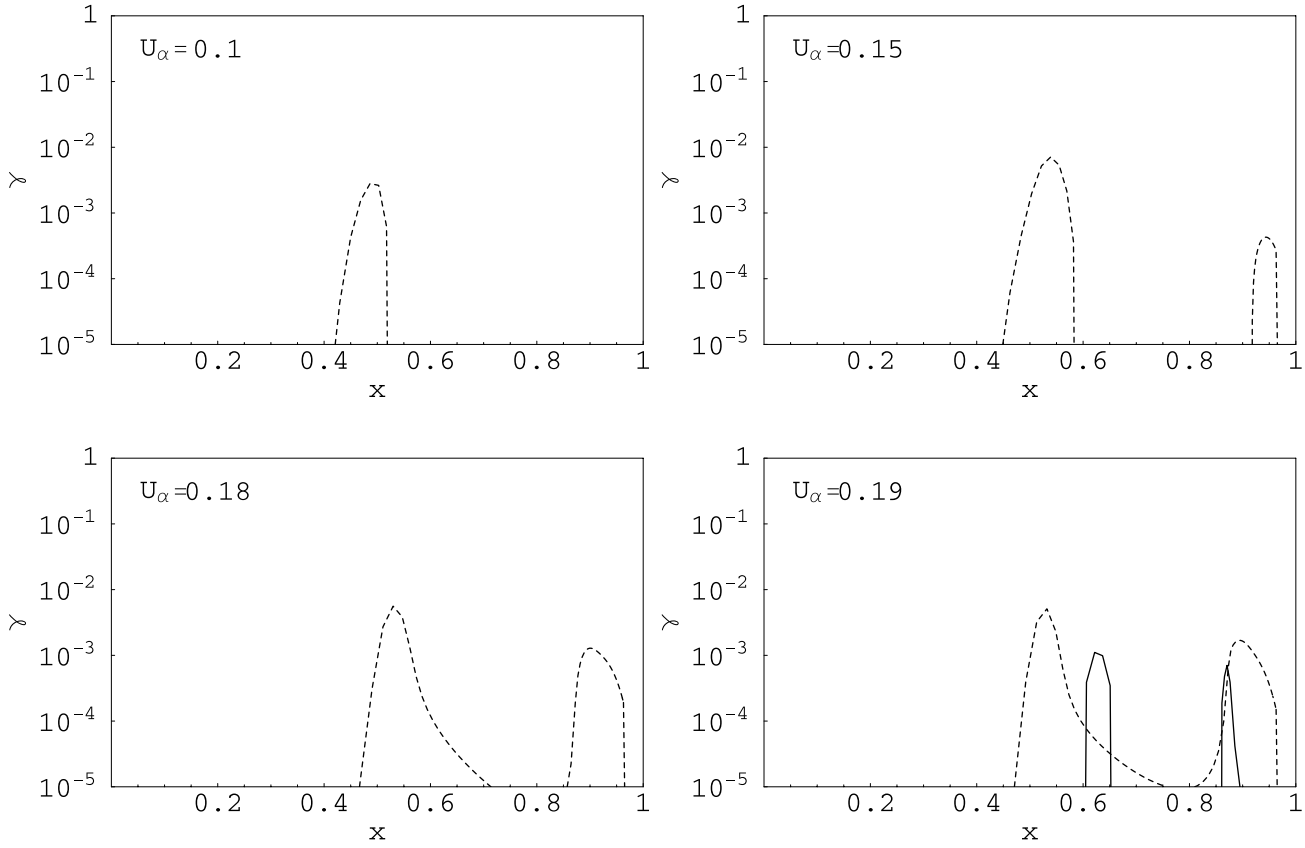

Figure 11. Growth rate versus x for the case of Figure 7, but for $U_{O^{+6}} = 0.2$ and (a) $U_\alpha = 0.1$, (b) $U_\alpha = 0.15$, (c) $U_\alpha = 0.18$, (d) $U_\alpha = 0.19$. The unstable roots are (R2), solid line, and (R3), dotted line.

where β_p becomes much larger than 10^{-4}, from Figure 2b it follows that the proton-cyclotron instability is completely stabilized (for $A_\alpha = 6$) and, therefore, this is an unlikely mechanism for proton-cyclotron wave generation at such distances.

[32] **Acknowledgments.** This work has been partially supported by FONDECYT grant 1020152 and FONDECYT grant 1000808.

References

Axford, W. I., and J. F. Mckenzie, The origin of the high speed solar wind streams, in *Solar Wind Seven*, edited by E. Marsch and R. Schwenn, pp. 1–5, Oxford Univ. Press, New York, 1992.

Axford, W. I., and J. F. McKenzie, Acceleration of the solar wind, in *Solar Wind Eight*, *AIP Conf. Proc.*, edited by D. Winterhalt et al., pp. 382, Pergamon, New York, 1996.

Cranmer, S. R., Ion cyclotron wave dissipation in the solar corona: The summed effect of more than 2000 ion species, *Astrophys. J.*, *532*, 1197, 2000.

Cranmer, S. R., et al., An empirical model of a polar coronal hole at solar minimum, *Astrophys. J.*, *511*, 481, 1999a.

Cranmer, S. R., G. B. Field, and J. L. Kohl, Spectroscopic constraints on models of in-cyclotron resonance heating in the polar solar corona and high speed solar wind, *Astrophys. J.*, *518*, 937, 1999b.

Fried, B. D., and S. D. Conte, *The Plasma Dispersion Function*, Academic, San Diego, Calif., 1961.

Gary, S. P., L. Yin, D. Winske, and L. Ofman, Electromagnetic heavy ion cyclotron instability: Anisotropy constraint in the solar corona, *J. Geophys. Res.*, *106*, 10,715, 2001.

Gomberoff, L., Electrostatic waves in the Earth's magnetotail and in comets, and electromagnetic instabilities magnetosphere and the solar wind, *IEEE Trans. Plasma Sci.*, *20*, 843, 1992.

Gomberoff, L., and R. Elgueta, Resonant acceleration of alpha particles by ion-cyclotron waves in the solar wind, *J. Geophys. Res.*, *96*, 9801, 1991.

Gomberoff, L., and R. Neira, Convective growth rate of ion-cyclotron waves in a H^+-He^+, and H^+-He^+-O^+ plasma, *J. Geophys. Res.*, *88*, 2170, 1983.

Gomberoff, L., and J. A. Valdivia, Proton-cyclotron instability induced by the thermal anisotropy of minor ions, *J. Geophys. Res.*, *108*, doi:10.1029/2002JA009357, in press, 2003.

Gomberoff, L., and Vega, Effect of He^+ temperature and thermal anisotropy on the electromagnetic ion-cyclotron instability in the geosynchronous region of GEOS-2, *J. Geophys. Res.*, *92*, 7728, 1987.

Gomberoff, L., F. T. Gratton, and G. Gnavi, Acceleration and heating of heavy ions by circularly polarized Alfvén waves, *J. Geophys. Res.*, *101*, 15,661, 1996.

Hollweg, J. V., and S. A. Markovskii, Cyclotron resonances of ions with obliquely propagating waves in coronal holes and the fast solar wind, *J. Geophys. Res.*, *107*(A6), 1080, doi:10.1029/2001JA000205, in press, 2002.

Hu, Y. Q., and S. R. Habbal, Resonant acceleration and heating of solar wind ions by dispersive ion cyclotron waves, *J. Geophys. Res.*, *104*, 17,045, 1999.

Isenberg, P. A., The kinetic shell model of coronal heating and acceleration by ion cyclotron waves, *J. Geophys. Res.*, *106*, 29,249, 2001.

Isenberg, P. A., and J. V. Hollweg, On the preferential acceleration and heating of the solar wind heavy ions, *J. Geophys. Res.*, *88*, 3923, 1983.

Isenberg, P. A., M. A. Lee, and J. V. Hollweg, The kinetic shell model of coronal heating and acceleration by ion cyclotron waves, *J. Geophys. Res.*, *106*, 5649, 2001.

Kohl, J. L., et al., UVCS/SOHO empirical determinations of anisotropic velocity distributions the solar corona, *Astrophys. J.*, *501*, L127, 1998.

Kohl, J. L., et al., EUV spectral line profiles in polar coronal hole from 1.3 to 3.0 solar radii, *Astrophys. J.*, *510*, L59, 1999a.

Kohl, J. L., et al., UVCS/SOHO observations of spectral line profiles in polar coronal holes, *Space Sci. Rev.*, *87*, 233, 1999b.

Leamon, R. J., W. H. Matthaeus, C. W. Smith, G. P. Zank, D. J. Mullan, and S. Oughton, MHD-driven kinetic dissipation in the solar wind and corona, *Astrophys. J.*, *537*, 1054, 2001.

Lee, L. C., A new mechanism of coronal heating, *Space Sci. Rev.*, *95*, 95, 2001.

Lee, L. C., and B. H. Wu, Heating and acceleration of protons and minor ions by fast shocks in the solar corona, *Astrophys. J.*, *537*, 535, 2000.

Li, X., and S. Habbal, Damping of fast and ion-cyclotron oblique waves in the multi-ion fast solar wind, *J. Geophys. Res.*, *106*, 10,669, 2001.

Li, X., S. R. Habbal, J. Kohl, and G. Noci, The effect of temperature anisotropy on observations of doppler dimming and pumping in the inner corona, *Astrophys. J.*, *501*, L133, 1998.

Li, X., S. R. Habbal, J. V. Hollweg, and R. Esser, Heating and cooling of protons by turbulence-driven ion cyclotron waves in the fast solar wind, *J. Geophys. Res.*, *104*, 2521, 1999.

Markovskii, S. A., Generation of ion cyclotron waves in corona holes by a global resonant magnetohydrodynamic mode, *Astrophys. J.*, *557*, 337, 2001.

Marsch, E., Close of multi-fluid and kinetic equations for cyclotron-resonant interactions of solar wind ions with Alfvén waves, *Nonlinear Process. Geophys.*, *5*, 11, 1998.

Ofman, L., A. Vinas, and S. P. Gary, Constraints on the O^{+5} anisotropy in the solar corona, *Astrophys. J.*, *547*, L175, 2001.

Tu, C. Y., and E. Marsch, MHD structures, waves, and turbulence in the solar wind, *Space Sci. Rev.*, *73*, 1, 1995.

Tu, C. Y., and E. Marsch, Study of the heating mechanism of the solar wind in coronal holes, in *Solar Wind Nine*, *AIP Conf. Proc.*, vol. 471, edited by S. R. Habbal et al, pp. 373, Woodbury, New York, 1999.

Tu, C. Y., and E. Marsch, Cyclotron wave heating and acceleration, *J. Geophys. Res.*, *106*, 8233, 2001.

L. Gomberoff and J. A. Valdivia, Departamento de Física, Facultad de Ciencias, Universidad de Chile, Casilla 653, Santiago, Chile. (lgombero@uchile.cl; alejo@fisica.ciencias.uchile.cl)